Available online at www.sciencedirect.com
SCIENCE DIRECT®
Journal of Nuclear Materials 329–333 (2004) 874–879
journal of nuclear materials
www.elsevier.com/locate/jnucmat

Tritium profile in plasma-facing components following D–D operation

K. Sugiyama [a,*], T. Tanabe [a], K. Miyasaka [a], K. Masaki [b], K. Tobita [b], N. Miya [b], V. Philipps [c], M. Rubel [d], C.H. Skinner [e], C.A. Gentile [e], T. Saze [f], K. Nishizawa [f]

[a] *Department of Nuclear Engineering, Graduate School of Engineering, Nagoya University, Furo-cho, Chikusa-ku, Nagoya 464-8603, Japan*
[b] *Japan Atomic Energy Research Institute, Naka Fusion Facilities, Naka-machi, Naka-gun, Ibaraki 311-0193, Japan*
[c] *Institute of Plasma Physics, Forschungszentrum Jülich, Association, EURATOM, Trilaterial Euregio Cluster, 52425 Jülich, Germany*
[d] *Alfvén Laboratory, Royal Institute of Technology, Association EURATOM-VR, S-100 44 Stockholm, Sweden*
[e] *Princeton Plasma Physics Laboratory, Princeton, NJ 08543, USA*
[f] *Radioisotope Center, Nagoya University, Furo-cho, Chikusa-ku, Nagoya 464-8603, Japan*

Abstract

We have investigated the tritium depth profile near the surface of the limiter/divertor tiles used in the deuterium fueled machines, such as TEXTOR, TFTR and JT-60U by means of the imaging plate technique and a tritium survey monitor. Tritium depth profiles near the surface of the sample tiles were estimated by comparing the experimental results to a calculation using a 3-D Monte-Carlo code. In every sample tile, there was little tritium in the range from the surface to 1 μm depth. In contrast, tritium density tended to increase beyond 1 μm depth. These results indicate that the tritium retained near the surface was easily removed by isotope exchange with a deuterium plasma or various other tritium removal operations. On the other hand, such operations did not remove tritium retained beyond 1 μm depth, and this could be a potential issue in a next D–T machine.

PACS: 52.40.Hf

1. Introduction

In D–T reactors, not only D–T reactions but also D–D reactions occurs simultaneously. The cross-section of D–D reaction is approximately 1/100 of D–T reaction at 10 keV, a typical plasma temperature in ITER. The D–D reaction produces a triton with energy of 1 MeV, much higher than the plasma temperature. Several recent studies on the behavior of highly energetic ions have pointed out that some of the energetic ions, including tritons, can escape from the magnetic confinement field without fully losing their initial energy [1,2]. Tritons escaping from a plasma could be implanted deeply in the plasma-facing wall. Therefore, it is assumed that there are two processes of tritium retention in plasma-facing materials (PFM), which are (i) implantation of high energy tritons into the PFMs and (ii) co-deposition with eroded materials making a:C/H layers on the surface of the PFMs. For D–T machines, tritium was also found in the redeposition on the remote area or dust in the vessel [3–7].

The imaging plate (IP) technique has clearly shown a different tritium surface retention pattern in D–D machines, compared to those of the D–T machines. The

* Corresponding author. Tel.: +81-52 789 5135; fax: +81-52 789 5137.
E-mail address: h022413m@mbox.nagoya-u.ac.jp (K. Sugiyama).

0022-3115/$ - see front matter © 2004 Published by Elsevier B.V.
doi:10.1016/j.jnucmat.2004.04.345

surface radioactivity apparent on the limiter/divertor tiles exposed to D–D discharges was higher in the eroded region than in the redeposited region [6,7].

In this paper, the results of IP measurements of plasma-facing tiles used in D–D discharge machines, such as TEXTOR-94, TFTR and JT-60U, are summarized. In addition, tritium depth profiles near the surfaces of the tiles, which were obtained from an advanced IP method and tritium survey monitor measurements, are presented. From these results, tritium retention issues in D–D machines are discussed in comparison to D–T machines.

2. Experimental

In order to obtain the surface tritium activities of plasma-facing components, we have used the IP, which is a two-dimensional radiation detector having high resolution and the high sensitivity for tritium detection. A tritium image is obtained by placing the IP plus a thin film in contact with a tile. After exposure, IP readout gives photon-stimulated-luminescence (PSL) intensity pattern that is proportional to the energy deposition by beta particles impinging on the IP surface. Detailed description of the IP technique is available elsewhere [8–10]. The IP used here was BAS-TR2025, manufactured by Fuji Co. Ltd. for tritium detection.

We have also used a tritium survey monitor, TPS-303 (manufactured by ALOKA Co. Ltd.), which is a gas-flow type handheld counter designed especially to detect low level energy radiation sources such as ^{3}T or ^{14}C, and counts the number of photons induced by beta particles passing through a micron-thin film ($\sim$0.15 mg/cm^2) on the detection window (window size; 3 cm $\times$ 15 cm).

Fig. 1 shows the photographs of sample tiles, including (a) an advanced limiter tile (ALT-II) from the poloidal belt limiter in TEXTOR-94 (ALT-II), (b) a limiter tile (RB12) installed in the mid-plane of the TFTR bumper limiter, and (c) a dome top tile (7DM5bp/bq) from the W-shaped divertor in JT-60U. All samples were used in the D–D discharge operation phase of each device.

For depth profiling of tritium, we have employed the film insertion method, where thin films of various thicknesses were inserted between the tile surface and the detector, and the attenuation of detected signal intensity by the shielding effects of the inserted film was obtained as a function of the inserted film thickness. The films were manufactured by Toray Industrial Inc., with the thinnest film of 1.2 μm ($\sim$0.16 mg/cm^2) in thickness. The film insertion method was applied both for IP measurement and the survey monitoring. A brief description on the estimation of the depth distribution from the attenuation curves is given in Section 3.2.

3. Result

3.1. Experimental results

Fig. 1 shows the IP images of the sample tiles together with their photographs. A higher tritium level is shown in red and a lower level in blue. [1] The ALT-II tile image (Fig. 1(a)) shows a typical tritium distribution found in D–D tiles: the tritium intensity of the redeposition-dominant region on the upper part of the tile was low, while the tritium distribution was rather homogeneous with higher intensity in the erosion-dominated regions (as mentioned in Section 1). Interestingly, it was found that the tritium intensity in the tile substrate beneath the redeposited layer was equal or higher than that of the eroded region [8,11]. As seen in Fig. 1(b), the TFTR bumper limiter tile image is very complicated because of the deposition of some contaminants on the tile surface. On the dome top tile of JT-60U (Fig. 1(c)), where no continuous redeposited layer was found [12], the tritium distribution was comparatively homogeneous in the toroidal direction, similar to the erosion-dominant area of the ALT-II limiter in TEXTOR.

Fig. 2 shows the attenuation curves of normalized PSL intensities, as a function of inserted film thickness, for the eroded region where tritium distribution was nearly homogeneous. The attenuation curves for tiles used in TFTR and JT-60U were very similar, while the TEXTOR tile showed a steeper decrease than the other two tiles.

Another attenuation curve obtained by the survey monitor measurement is shown in Fig. 3. According to the Katz–Penfold's equation [13], the range of 19 keV beta electrons produced by tritium beta-decay is about 0.6 mg/cm^2. Therefore, the initial significant attenuation found in $\sim$0.6 mg/cm^2 is mainly caused by the shielding of the beta electrons from tritium in the sample tiles, and the counts seen around 0.6 mg/cm^2 thickness should reflect the beta electrons generated at the surface of the tiles. The background level remained with the insertion of a very thick film was due to other radiation sources producing much higher energy electrons and/or gamma-rays such as ^{7}Be, ^{60}Co and others.

3.2. Estimation of tritium depth profile

Here we describe the method of tritium depth profiling from the attenuation curve. Let $D(x)$ be a tritium depth profile, where x is the depth from the surface. Some of the beta electrons from tritium at the depth x can escape from the surface and reach to the detector through the shielded film. The number of beta electrons

[1] For interpretation of color in Fig. 1, the reader is referred to the web version of this article.

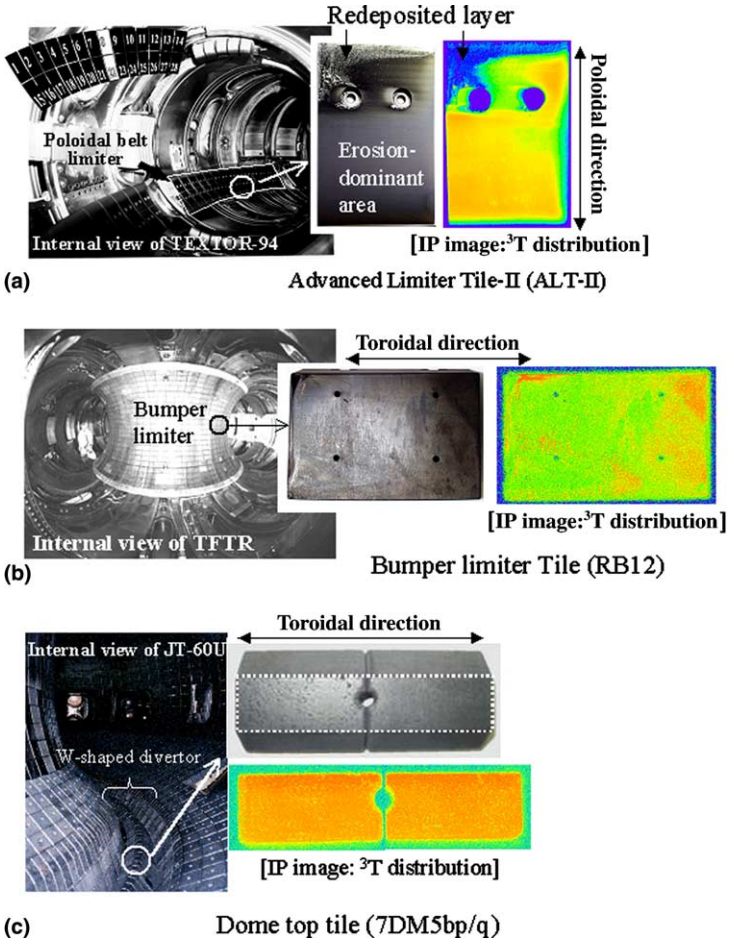

Fig. 1. The photographs and tritium images of sample tiles. (a) Internal view of TEXTOR-94 vacuum vessel and sample: ALT-II graphite tile installed in poloidal belt limiter. There was redeposited layer on the upper region of ALT-II tile, where tritium level was rather low. (b) Internal view of TFTR and sample: bumper limiter graphite tile (RB-12). Since some dust-like depositions were found on the surface of RB12 tile, image is not so clear unfortunately. (c) Internal view of JT-60U, photograph of W-shaped divertor and sample: dome top tile (7DM5bp/q:CFC) which is one of the regions where highest tritium level was found. Toroidal tritium distribution was comparatively homogeneous.

which can be detected by IP or the survey monitor is thus expressed as $k(x,a)D(x)$, where the coefficient $k(x,a)$ is the probability for an electron generated at depth x in graphite and penetrating through the shielded film of thickness a without completely losing its energy. Hence, the count of beta particles detected by the survey monitor shielded by inserting a film of thickness 'a' is given as

$$C(a) = \int_0^{xL(a)} k(x,a)D(x)\mathrm{d}x, \tag{1}$$

where $xL(a)$ is the detection limit in depth, which varies with the thickness of the film, a.

In the case of the IP measurement, the energy of the escaping beta electron is an additional factor because PSL intensity is proportional to the deposited energy in IP. Then, PSL intensity is expressed as function of film thickness, a

$$\mathrm{PSL}(a) = \int_0^{xL(a)} \int_0^{\infty} Q(E,x,a)k(x,a)D(x)E\mathrm{d}E\mathrm{d}x, \tag{2}$$

where $Q(E,x,a)$ is the energy distribution of escaping electrons, and $Q(E,0,0)$ is the initial energy spectrum corresponding to the tritium beta energy spectrum [15].

In this estimation, $k(x,a)$, $Q(E,x,a)$ and $xL(a)$ were calculated by using MCNP code [14] which can simulate the three-dimensional transport of photon/electron/neutron in the materials by Monte-Carlo method. The optimal function $D(x)$ was determined such that $\mathrm{PSL}(a)$ and $C(a)$, which are the convolution of $D(x)$ and the

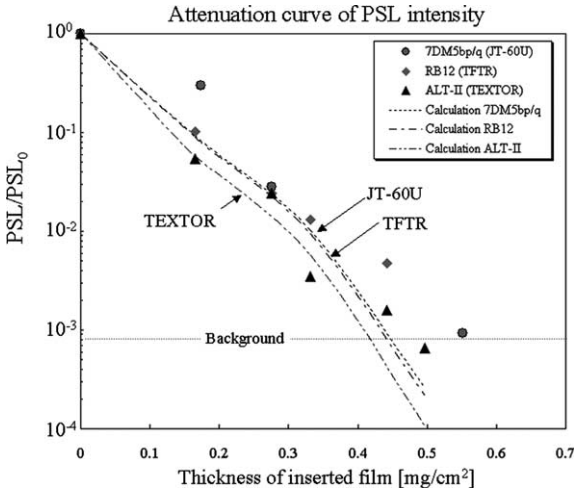

Fig. 2. The attenuation curves of normalized PSL intensity (PSL/PSL_0) as function of shielding film thickness obtained by IP measurement. Here, PSL_0 is PSL intensity without any film insertion. The ALT-II sample from TEXTOR shows steeper decrease than other two samples. The dotted lines overlaid on the each plots are the expected ones derived from the estimated depth profiles: $D(x)$.

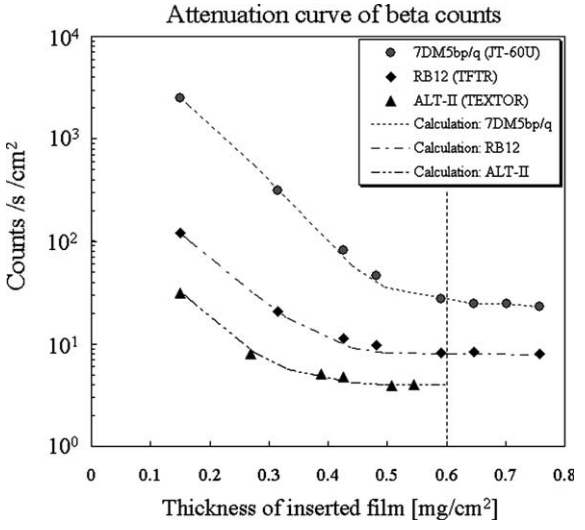

Fig. 3. The beta cpm (beta particle counts per minute) attenuation curves obtained by survey monitor measurement. The dotted lines overlaid on the each plots are the expected ones derived from the estimated depth profiles: $D(x)$.

calculated $k(x,a)$ and $Q(E,x,a)$, reproduce the experimental attenuation curves.

Fig. 4 shows the depth profile, $D(x)$, thus derived. The dotted lines overlaid on the experimental plots in Figs. 2 and 3 are expected $C(a)$ and $\mathrm{PSL}(a)$ (expressed as $\mathrm{PSL}(a)/\mathrm{PSL}(0)$ in the figure) for each depth profile. One can note very low tritium retention within 1 μm

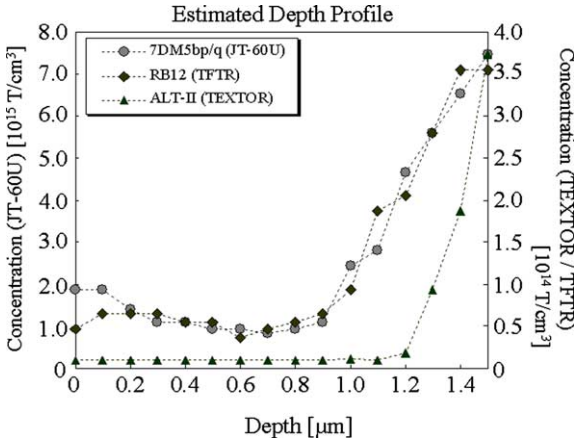

Fig. 4. The estimated depth profiles of the region from top surface to 1.5 μm depth. All sample show that little tritium retention within 1 μm depth from the surface.

from the surface. Beyond 1 μm in depth, however, tritium density starts to increase significantly with the depth. Unfortunately, however, we could not get the profiles deeper than 1.5 μm because of diminishing of the escaping tritium betas. According to TRIM code [16] calculation, the range of 1 MeV triton in graphite at normal incidence is about 10 μm. Taking various incident angles due to gyration in magnetic field into account, tritium could be present up to 10 μm in depth. Actually, in the first wall of JET, tritium was detected even at 8.5 μm in depth [17].

4. Discussion

In current tokamaks with carbon materials used as PFM, hydrogen/deuterium (H/D) is retained mostly in co-deposited carbon layers. Even tritium in JET and TFTR during their D–T campaign behaved similar to H/D. Accordingly, it was expected that tritium produced in D–D machines should have behaved similar to deuterium, because even high energy triton was thought to lose its energy in the deuterium plasma. However, as shown in the present and previous papers, tritium distribution on PFM in the D–D machines is quite different from that of deuterium. In particular, on the ALT tile of TEXTOR the tritium distribution is different to deuterium which was retained mostly in redeposited layers (see Fig. 1(a) and Ref. [18]). This is because high energy triton is implanted in to the beyond a 1 μm in depth, while (H/D) is retained in carbon deposited layers.

Applications of Monte-Carlo simulation codes for the behavior of energetic triton in tokamaks such as the ORBIT/TRANSP code in TFTR and the OFMC code in JT-60U have already shown that high energy triton can escape from the plasma by the orbit loss and ripple

loss mechanisms and be implanted in plasma-facing surfaces [19–21]. In JT-60U, the OFMC code has indicated that about 30% of total tritons produced were implanted with energy of more than 500 keV [21]. Moreover, the tritium distribution observed by the IP reflects higher energetic tritons escaping at baffle plates, mid-plane of the first wall, and the dome top with toroidal periodicity due to magnetic ripple loss mechanism [22]. The analysis of D–D tritons carried out in TFTR also showed that experimental results were roughly consistent with numerical results [23].

Nevertheless, not a small amount of the total tritons produced must be thermalized in plasma and behave similarly to protium and deuterium. This raises the question why tritium was not retained in shallower region in the D–D tiles. Since plasma-facing walls are always subjected to deuterium plasma at 10^{18}–10^{19} D cm^2/s during discharges, tritium even once retained near the surface can be immediately replaced by deuterium. This is supported by SIMS analysis for the dome top tile of JT-60U, which showed that the majority of retained hydrogen isotope in the region within about 1 μm depth was deuterium [24]. Various wall-cleaning operations and/or hydrogen discharges carried out in each device also removed the tritium retained near the surface.

Finally, we would like to point out that high energetic triton implantation could contribute to long-term tritium inventory in D–T machines. Because (i) the deeply implanted tritium in PFM cannot be easily replaced by D injecting to the surface, (ii) compared to shallower region where should be saturated with D/T, the concentration of deeply implanted tritium could increase up to (T+D)/C∼0.4 in the long-term. In addition, the area where high energetic triton can be implanted is not necessarily the same to the carbon deposited area. Taking the operational parameters of ITER into consideration, not only in D–D phase but also in D–T phase, approximately 10^{17} tritons/s will be produced by D–D reactions. Extrapolating from JT-60U case [21] where the flux of those tritons becomes ∼10^{12} T/cm^{2}s on the private region or outer baffle area, long duration discharge such as 1000 s/pulse can cause several kBq/cm^2 tritium retention per pulse. Of course, in ITER or a reactor, energetic triton must deposit its energy into the plasma due to the higher magnetic field and plasma current than the present machines, otherwise no alpha-heating is possible. The above number could be somewhat overestimated.

5. Conclusion

In order to investigate the accumulation of tritium in the plasma-facing walls of D–D machines, tritium retention and depth profiles of the limiter/divertor tiles used in the D–D machines (TEXTOR, TFTR and JT-60U) were measured by the IP technique and a survey monitor.

It was found that little tritium was retained within 1 μm depth from the surface of the tiles. However, tritium retention was appreciable beyond 1 μm in depth. This leads us to conclude that a large amount of tritons produced by D–D reactions can penetrate deeply into the plasma-facing tiles without fully losing their initial energy, while tritons that are thermalized in the plasma are retained in the surface layers and can be easily replaced by deuterium in the plasma or be removed by a number of wall-cleaning operations. In contrast, the tritium that is deeply implanted may be more difficult to remove.

In next-generation D–T reactors, the main issue of tritium retention is co-deposition of tritium with eroded materials. The deeply implanted tritium which is hard to remove can also be a long-term potential issue. We might need to develop a method to remove deep implanted tritium as well as to remove co-deposited tritium on the surface.

References

[1] W.W. Heidbrink, G.J. Sadler, Fus. Eng. Des. 34 (1994) 535.
[2] K. Tobita, S. Nishio, S. Konishi, et al., Fus. Eng. Des. 65 (2003) 561.
[3] J.P. Coad, N. Bekris, J.D. Elder, et al., J. Nucl. Mater. 290–293 (2001) 224.
[4] A.T. Peacock, P.A. Andrew, D. Brennan, et al., Fus. Eng. Des. 49&50 (2000) 745.
[5] C.H. Skinner, C.A. Gentile, G. Ascione, et al., J. Nucl. Mater. 290–293 (2001) 486.
[6] T. Tanabe, N. Bekris, J.P. Cord, et al., J. Nucl. Mater. 313–316 (2003) 478.
[7] K. Sugiyama, K. Miyasaka, T. Tanabe, et al., J. Nucl. Mater. 313–316 (2003) 507.
[8] K. Miyasaka, T. Tanabe, G. Mank, et al., J. Nucl. Mater. 290–293 (2001) 448.
[9] T. Tanabe, K. Miyasaka, M. Rubel, et al., Fus. Sci. Technol. 41 (2002) 924.
[10] Y. Amemiya, J. Miyahara, Nature (Loud.) 336 (1988) 89.
[11] T. Tanabe, V. Philipps, Fus. Eng. Des. 54 (2001) 147.
[12] Y. Gotoh, J. Yagyu, K. Masaki, et al., J. Nucl. Mater. 313–316 (2003) 370.
[13] L. Katz, A.S. Penfold, Rev. Mod. Phys. 24 (1952) 28.
[14] Judith F. Briesmeister, MCNP – A general Monte Carlo N-particle transport code, Los Alamos National Laboratory report LA-12625-M, 1993.
[15] P.C. Souers, Hydrogen Properties for Fusion Energy, University of California, 1986.
[16] J.F. Ziegler, J.P. Biersack, U. Littmark, The Stopping and Range of Ions in Solids, Pergamon, New York, 1985.
[17] C. Stan-sion, R. Behrisch, J.P. Coad, et al., J. Nucl. Mater. 290–293 (2001) 491.
[18] M. Rubel, P. Wienhold, D. Hildebrandt, J. Nucl. Mater. 290–293 (2001) 473.

[19] S.J. Zweben, D.S. Darrow, H.W. Herrmann, et al., Nucl. Fus. 35 (1995) 893.
[20] S.J. Zweben, D.S. Darrow, H.W. Herrmann, et al., Measurements of DT alpha particle loss near the outer midplane of TFTR' PPPL report-3118, 1995.
[21] K. Masaki, K. Sugiyama, T. Tanabe, et al., J. Nucl. Mater. 313–316 (2003) 514.
[22] K. Sugiyama, T. Tanabe, K. Masaki, et al., Phys. Scr. T103 (2003) 56.
[23] R. Bastasz, D. Buchenauer, S. Zweben, Rev. Sci. Instrum. 61 (1990) 3199.
[24] Y. Hirohata, Y. Oya, H. Yoshida, et al., Phys. Scr. T103 (2003) 15.